

Plasmonic-modulated dissipative-driven multiqubit entanglement under asymmetric detuningWeichen Tang , Feng Lin, Xing Zhu, and Zheyu Fang ^{*}*School of Physics, State Key Lab for Mesoscopic Physics, Academy for Advanced Interdisciplinary Studies, Collaborative Innovation Center of Quantum Matter, and Nano-optoelectronics Frontier Center of Ministry of Education, Peking University, Beijing 100871, China*

(Received 31 July 2019; revised manuscript received 8 October 2019; published 23 October 2019)

A dissipative-driven system can generate steady-state entanglement robust to control parameters, while a quantum plasmonic system has the advantages of being strongly coupled to qubits and manipulation of electromagnetic waves in the subwavelength regime. We propose an effective multiqubit dissipative-driven entanglement model for a plasmonic system which takes into account coupling of the plasmonic cavity and qubits as well as the direct coupling between any two qubits and develop a numerical solution of the effective model on a scalable composite plasmonic structure. In this structure, the multiqubit entanglement under asymmetric detuning, especially for those combinations containing pairs of antisymmetric detuning qubits, achieves stronger steady-state entanglement measured by negativity and pairwise concurrence. The robustness of multiqubit entanglement against variations of the control parameters is also presented. In addition, the phenomenon of entanglement sudden death caused by the driving field in entanglement dynamics is investigated. Our model shows evidence that quantum plasmonics has great potential in multiqubit entanglement.

DOI: [10.1103/PhysRevB.100.165415](https://doi.org/10.1103/PhysRevB.100.165415)**I. INTRODUCTION**

Quantum entanglement plays a fundamental role in quantum information and quantum computation, such as quantum logic gates, quantum encryption, and quantum error correction [1–4]. However, entanglement could hardly be achieved due to the weak direct interaction between qubits. To overcome this limitation, several methods have been proposed, for example, nonlinear optical crystals, nuclear magnetic resonance, etc. [1,5–7]. Quantum plasmonic structures possess unique advantages in strong coupling and a smaller size which can go beyond optical limit [8–12].

Recent study has focused on two-qubit entanglement, while the study of multiqubits has gradually attracted attention. González-Tudela *et al.* [13–15] investigated a series of systems which generate entanglement from two qubits to multiple equidistant arranged isomorphic qubits by a plasmonic waveguide and found that four-level system is more robust than two-level system. Mirza and Schotland [16] analyzed multiqubit transient entanglement in a bidirectional waveguide and discovered that both entanglement time and maximum entanglement could increase at least by 3/2 with the chiral waveguide. In addition to waveguides, other plasmonic structures such as metallic nanospheres and nanoantennas have also been studied. Ren *et al.* [17] derived an analytical solution for entanglement of two to four qubits induced by multinanospheres with Green's tensor technique. Otten *et al.* [18–20] focused on the effect of the coupling constant on entanglement and provided both numerical and analytical solutions when the spontaneous vacuum emission of qubits could be ignored. In summary, current research on

multiqubit entanglement often involves some simplifications, such as considering a one-dimensional condition or ignoring the dissipation.

However, the duration of those entanglements could hardly exceed the picosecond level when all the dissipation is taken into account. In order to be more easily verified by experiment and better applied, other methods to prolong entanglement have been studied. One of them is dissipative-driven entanglement (DDE), where the entanglement is stabilized and irrelevant of the initial state. In other words, the steady-state entanglement is decided only by the control parameters of the system. Another advantage of DDE is that it fits well with the plasmonic structure whose loss is strong and unavoidable [21]. Under the condition of strong plasmonic dissipation, several effective models for a two-qubit system were proposed [22–24]. Thereby, some effects of control parameters on entanglement were discovered, such as the fact that maximum entanglement could be obtained with the symmetric coupling constant [22] and the symmetric driving field [23].

At present, DDE research is limited to two-qubit entanglement, and due to computational complexity, multiqubit DDE is still under investigation. In addition, as the number of qubits increases, the number of control parameter combinations increases exponentially; thus, in a multiqubit entanglement simulation, the control parameters are usually set to be symmetric among different qubits. However, previous studies [24,25] have shown that the asymmetry of the control parameters, especially asymmetric detuning, plays an important role in the two-qubit system. Therefore, asymmetric detuning needs to be paid attention to in multiqubit entanglement. In addition, although the driving field is one of the keys to maintaining steady-state entanglement [26,27], its influence on multiqubit entanglement dynamics has not been fully revealed.

^{*}zhyfang@pku.edu.cn

To address these issues, an efficient multiqubit system model is proposed to reduce computational complexity. A scalable plasmonic system consisting of a multiqubit and a dissipative nanoparticle is designed to generate multiqubit DDE. The numerical simulation of the plasmonic system by the effective model demonstrates that the steady-state entanglement produced by the nonzero asymmetric detuning is significantly larger than that at resonance. In addition, the number of pairs of antisymmetric detuning qubits plays an important role in entanglement enhancement, and the maximum entanglement can be obtained by appropriately combining the control parameters. Meanwhile, entanglement under small parameter variations has proven to be robust, which preserves the properties of DDE. Last, it is observed that a sufficiently strong driving field may cause entanglement sudden death (ESD) in the dynamics of multiqubit entanglement.

II. THEORY

A. Lindblad equation and effective model

The proposed plasmonic system consists of a multiqubit and a dissipative nanoparticle, driven by a classical field, $E = E_0 e^{i\omega t} + \text{c.c.}$ A possible physical realization is illustrated in Sec. II B. The Hamiltonian of the nanoparticle near a resonance mode ω_a can be described as $H_c = \omega_a a^\dagger a$, where a^\dagger (a) is the bosonic creation (annihilation) operator of the surface plasmon mode. Each qubit is a two-level system, and the Hamiltonian for the i th qubit is $H_i = \omega_i \sigma_i^\dagger \sigma_i$, where σ_i^\dagger (σ_i) is the raising (lowering) operator and ω_i is the energy level difference. We define $d_a = a^\dagger + a$ and $d_i = \sigma_i^\dagger + \sigma_i$ to be the dipole operators of the cavity and qubits. The Hamiltonian for dipole-dipole coupling is $H_I = \sum_i g_i d_a d_i + \sum_{i < j} J_{ij} d_i d_j$, where g_i is the coupling constant between the i th qubit and the cavity and J_{ij} is the coupling constant between the i th and j th qubits. The last term, $H_D = -\sum_i \eta_i d_i + \eta_a d_a$, denotes the interaction between the driving field and the system. The total Hamiltonian of the system in the corotating reference under the rotation wave approximation is

$$H = \Delta_a a^\dagger a + \sum_{i=1}^n \Delta_i \sigma_i^\dagger \sigma_i - \eta_a (a^\dagger + a) - \sum_{i=1}^n \eta_i (\sigma_i^\dagger + \sigma_i) - \sum_{i=1}^n g_i (\sigma_i^\dagger a + \sigma_i a^\dagger) - \sum_{\substack{i,j=1 \\ i < j}}^n J_{ij} (\sigma_i^\dagger \sigma_j + \sigma_i \sigma_j^\dagger), \quad (1)$$

where n is the number of qubits. $\Delta_a = \omega_a - \omega$ denotes the detuning between the cavity and the driving field, and $\Delta_i = \omega_i - \omega$ is the detuning between the i th qubit and the driving field. $\eta_i = \mu_i E_0$ and $\eta_a = \mu_a E_0$ are the Rabi frequency of the qubits and cavity, while μ_i and μ_a represent their dipole moments.

Dissipation of the system is modeled by Lindblad's master equation (ρ is the density matrix of the whole system)

$$\dot{\rho} = i[\rho, H] + \Gamma(\rho), \quad (2)$$

where $\Gamma(\rho)$ denotes the decay term. Assume the vacuum spontaneous emission rate for the i th qubit is γ_i and the decay

rate for the nanoparticle is γ_a ; the decay term is

$$\Gamma(\rho) = \sum_{i=1}^n \frac{\gamma_i}{2} (2\sigma_i \rho \sigma_i^\dagger - \{\sigma_i^\dagger \sigma_i, \rho\}) + \frac{\gamma_a}{2} (2a \rho a^\dagger - \{a^\dagger a, \rho\}). \quad (3)$$

In order to eliminate the operators of the cavity, an effective model for the weak-detuning and weak-coupling regime ($g_i, \eta_i, \gamma_i, \Delta_i \ll \gamma_a$) is provided. Among different approaches [22–24] for a two-qubit system, we found that adiabatic elimination [22] could be generalized to a multiqubit system.

First, we begin with the Heisenberg picture of motion

$$\dot{\sigma}_i^z = 2i \left[\eta_i (\sigma_i^\dagger - \sigma_i) + \sum_{j \neq i} J_{ij} (\sigma_i^\dagger \sigma_j - \sigma_i \sigma_j^\dagger) + g_i (\sigma_i^\dagger a - \sigma_i a^\dagger) \right] - \gamma_i (\mathbf{1} - \sigma_i^z) + f_i^z, \quad (4)$$

$$\dot{\sigma}_i = -i \left[\left(\eta_i + g_i a + \sum_{j \neq i} J_{ij} \sigma_j \right) \sigma_i^z + \delta_i \sigma_i \right] - \frac{\gamma_i \sigma_i}{2} + f_i, \quad (5)$$

$$\dot{a} = i \left[\eta_a - \Delta_a a + \sum_i g_i \sigma_i \right] - \frac{\gamma_a a}{2} + f_a, \quad (6)$$

where σ_i^z is defined as $\sigma_i^z = [\sigma_i^\dagger, \sigma_i]$. f_i^z, f_i, f_a in Eqs. (4), (5), and (6) are fluctuation operators representing higher-order process [22]. Under the semiclassical approximation, the expectation values for those fluctuation operators are zero. In addition, when $\langle a \rangle$ varies slowly, which is valid in the weak-coupling regime, it is reasonable to set $\dot{a} = 0$ and obtain an expression for a as a function of σ_i ,

$$a = \frac{\eta_a + \sum_i g_i \sigma_i}{\Delta_a - i\gamma_a/2}. \quad (7)$$

Substituting the expression for a into Eqs. (4) and (5), we have Eq. (8), which can be viewed as the Heisenberg equation of operators for an effective Hamiltonian and dissipation term. The effective Hamiltonian is

$$H^{\text{eff}} = \sum_i [\tilde{\Delta}_i \sigma_i^\dagger \sigma_i - \tilde{\eta}_i (\sigma_i^\dagger + \sigma_i)] - \sum_{\substack{i,j=1 \\ i < j}}^n \tilde{J}_{ij} (\sigma_i^\dagger \sigma_j + \sigma_i \sigma_j^\dagger), \quad (8)$$

where the effective detuning, Rabi frequency, and coupling constant are

$$\begin{aligned} \tilde{\Delta}_i &= \Delta_i - \frac{g_i^2 \Delta_a}{\left(\frac{\gamma_a}{2}\right)^2 + \Delta_a^2}, \\ \tilde{\eta}_i &= \eta_i + \frac{g_i \Delta_a \eta_a}{\left(\frac{\gamma_a}{2}\right)^2 + \Delta_a^2}, \\ \tilde{J}_{ij} &= J_{ij} + \frac{g_i g_j \Delta_a}{\left(\frac{\gamma_a}{2}\right)^2 + \Delta_a^2}. \end{aligned} \quad (9)$$

Meanwhile, the effective dissipation term is

$$\Gamma^{\text{eff}}(\rho^{\text{eff}}) = \sum_{i,j=1}^n \frac{\tilde{\gamma}_{ij}}{2} [2\sigma_i \rho^{\text{eff}} \sigma_j^\dagger - \{\sigma_j^\dagger \sigma_i, \rho^{\text{eff}}\}], \quad (10)$$

where

$$\tilde{\gamma}_{ii} = \gamma_i + \frac{g_i^2 \gamma_a}{(\frac{\gamma_a}{2})^2 + \Delta_a^2}, \quad \tilde{\gamma}_{ij} = \frac{g_i g_j \gamma_a}{(\frac{\gamma_a}{2})^2 + \Delta_a^2}. \quad (11)$$

Therefore, an effective Lindblad equation is obtained,

$$\dot{\rho}^{\text{eff}} = i[\rho^{\text{eff}}, H^{\text{eff}}] + \Gamma^{\text{eff}}(\rho^{\text{eff}}), \quad (12)$$

for a multiqubit system with no plasmonic operators. Apparently, this effective model could decrease the dimension of the Hilbert space, thereby reducing the computational complexity and facilitating the entanglement simulation of more qubits. This model is used to obtain theoretical and numerical solutions in Sec. III.

B. Structure for a multiqubit and plasmonic system

Many different structures composed of waveguides, multiple qubits, and multiple nanospheres have been studied [17,18,28,29]; however, most of them are complicated and unscalable. Thus, a scalable structure that is a composite of only a metallic nanosphere and a multiqubit is designed, which is modified from a widely used structure in a two-qubit system [24,30].

As shown in Fig. 1, the dielectric constant of the metallic nanosphere is ϵ_m , and its radius is r_a . Qubits are located on a fixed plane passing through the center of the nanosphere. The distance between the i th qubit and the center of the nanosphere is r_i , and the distance between the i th and j th qubits is r_{ij} . The dipoles of qubits are all perpendicular to the plane (parallel to each other). The whole system is embedded in a host medium with dielectric constant ϵ_b .

For coupling constant in Eq. (1), g_i , can be determined by combining the classical Maxwell equation with quantum methods [5,31],

$$g_i = -\frac{\mu_i}{r_i^3} \sqrt{\frac{3\eta r_a^3}{4\pi\epsilon_0}}, \quad (13)$$

where μ_i is the dipole moment of the i th qubit, ϵ_0 is the vacuum dielectric constant, and $\eta^{-1} = d\text{Re}[\epsilon_m]/d\omega|_{\omega=\omega_a}$. J_{ij} is given by

$$J_{ij} = -\frac{\mu_i \mu_j}{4\pi\epsilon_0 \epsilon_b r_{ij}^3}. \quad (14)$$

In the interaction terms between the driving field and the system $\eta_i = \mu_i E$, $\eta_a = \mu_a E$, E is the strength of driving field, and μ_a is the dipole moment of the nanosphere,

$$\mu_a = \epsilon_b \sqrt{12\eta r_a^3 \pi \epsilon_0}. \quad (15)$$

If the dielectric constant of the host medium is $\epsilon_b = 3$ and the nanosphere is made of silver, $\gamma_a = 54.96$ meV could be derived from the imaginary part of ϵ_m [24]. The validity of the effective model requires that the detunings and couplings of qubits and the nanosphere are limited to the range $g_i, \eta_i, \gamma_i, \Delta_i \ll \gamma_a$. When $\Delta \sim \kappa$, the large detuning strongly

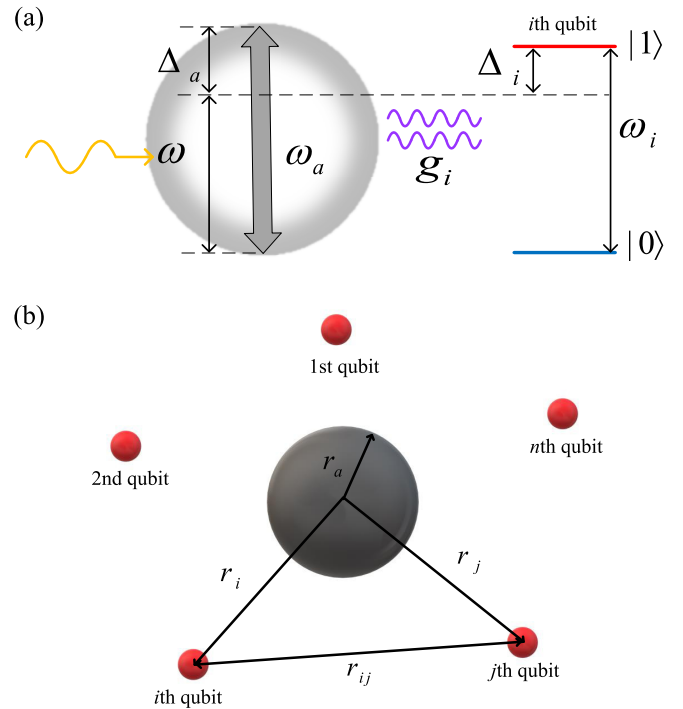


FIG. 1. Schematic diagrams of a system composed of multiple qubits (which could be molecules, atoms, or quantum dots) near a nanosphere along with (a) the energy levels of the system, the frequency of the driving field and (b) structural parameters. The qubits are on a fixed plane passing through the center of the nanosphere, and the number of qubits n can be adjusted. The whole system is embedded in a host medium with dielectric constant ϵ_b .

suppresses the entanglement, which is not considered here. The influence of those parameters under the weak-detuning and weak-coupling condition is discussed in Sec. III.

III. RESULTS AND DISCUSSION

Pairwise concurrence, which is widely used in multiqubit systems [16,18,19], is used to quantify the strength of entanglement. Concurrence [32] between two qubits is defined as

$$C(\rho_{ij}) = \max\{0, \lambda_1 - \lambda_2 - \lambda_3 - \lambda_4\}, \quad (16)$$

where ρ_{ij} is the reduced density matrix of the i th and j th qubits, which could be obtained by tracing out other qubits. λ_i are eigenvalues of $\sqrt{\rho_{ij} \tilde{\rho}_{ij}}$, where $\tilde{\rho}_{ij} = (\sigma_y \otimes \sigma_y) \rho_{ij}^* (\sigma_y \otimes \sigma_y)$, and $\sigma_y = \begin{pmatrix} 0 & -i \\ i & 0 \end{pmatrix}$ is the Pauli matrix.

However, even though concurrence performs well in a two-qubit system, it has been shown that there exists a three-qubit state, called the Greenberger-Horne-Zeilinger-like state, the is fully tripartite entangled while the concurrence of each pair of qubits is zero [33]. In order to identify the tripartite entangled state more precisely, negativity [34] is also chosen as a criterion. For a system composed of two subsystems A and B, the negativity of a state ρ with respect to A is defined as follows:

$$N_{A-B}(\rho) = -2 \sum_i \sigma_i(\rho^{TA}), \quad (17)$$

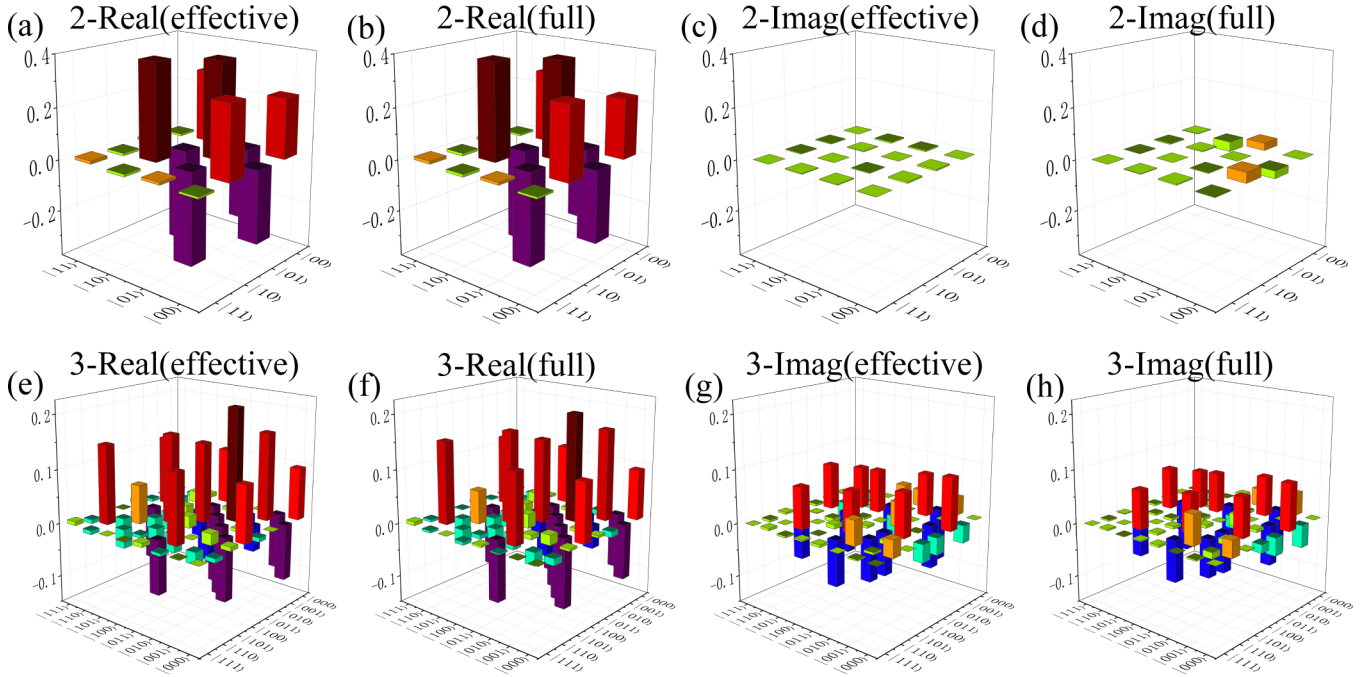


FIG. 2. Steady-state density matrix divided into (a), (b), (e), and (f) real elements and (c), (d), (g), and (h) imaginary elements for (a)–(d) two-qubit and (e)–(h) three-qubit systems. In (b), (d), (f), and (h) ρ^{full} is obtained from the original master equation, and in (a), (c), (e), and (g) ρ^{eff} is from the effective one. A strong match appears between both the real parts and imaginary parts of most matrix elements. The parameters are set as follows: $\eta_i = 1.6$ meV, $g_i = 0.34$ meV, $\gamma_i = 10$ μ eV, and $\gamma_a = 54.96$ meV in all panels and $\Delta_1 = -\Delta_2 = 1.2$ meV in (a)–(d) and $\Delta_1 = -\Delta_3 = 1.2$ meV, $\Delta_2 = 0$ in (e)–(h).

where $\{\sigma_i(\rho^{TA})\}$ are the negative eigenvalues of the partial transpose ρ^{TA} of ρ with respect to A, defined as $\langle i_A, k_B | \rho^{TA} | j_A, l_B \rangle = \langle j_A, k_B | \rho | i_A, l_B \rangle$. $N_{A-B}(\rho)$ greater than zero is a sufficient condition for A and B to be inseparable (entangled). For three-qubit systems, a fully tripartite entangled state is a state in which each of the three qubits is inseparable from the other two qubits. Thus, the tripartite negativity [33] of a three-qubit state is defined as

$$N_{ABC}(\rho) = (N_{A-BC} N_{B-AC} N_{C-AB})^{\frac{1}{3}}, \quad (18)$$

where A, B, and C each denote a qubit. Nonzero tripartite negativity is a sufficient condition for full tripartite entanglement. When the qubit number is greater than 3, it is generalized to the following form:

$$N_{A_1 A_2 \dots A_n}(\rho) = (N_{A_1 - A_2 \dots A_n} N_{A_2 - A_1 A_3 \dots A_n} \dots N_{A_n - A_1 \dots A_{n-1}})^{\frac{1}{n}}, \quad (19)$$

where A_1, A_2, \dots, A_n each denote a qubit. Even though nonzero negativity is not a sufficient condition for a fully entangled state, it still has significance: each qubit is inseparable from the other qubits. Therefore, the negativity defined in Eq. (19) is used to quantify the global entanglement of the multiqubit.

A. Verification of effective model

The validity of our effective model is evaluated by comparing the results of the full master equation (2) and the effective master equation (12). As our work focuses on the steady-state entanglement, it is necessary to compare only

the elements of the steady-state density matrix under typical parameters. We first consider the number of qubits $n = 2$. A detailed steady-state density matrix divided into real and imaginary parts is provided for both cases in Figs. 2(a)–2(d) under $\Delta_1 = -\Delta_2 = 1.2$ meV, $\eta_i = 1.6$ meV, $g_i = 0.34$ meV, $\gamma_i = 10$ μ eV, and $\gamma_a = 54.96$ meV. A great match is found between the real elements. Meanwhile, even though there are certain differences between the imaginary elements, those differences are tiny compared to the real elements, which means they would not affect the property of the whole density matrix.

Similarly, when the number of qubits $n = 3$, the real and imaginary parts of the steady-state density matrix are shown separately in Figs. 2(e)–2(h). The parameters are set as $\Delta_1 = -\Delta_3 = 1.2$ meV, $\Delta_2 = 0$, $\eta_i = 1.6$ meV, $g_i = 0.34$ meV, $\gamma_i = 10$ μ eV, and $\gamma_a = 54.96$ meV. Obviously, the weak-detuning and weak-coupling condition $g_i, \eta_i, \gamma_i, \Delta_i \ll \gamma_a$ is satisfied under these parameters, and both the real part and the imaginary part are also well matched. Thus, our effective model is verified at the density matrix level under the weak-detuning and weak-coupling condition. This model is used to investigate multiqubit entanglement in the following sections.

B. Steady-state entanglement under asymmetric detuning

As mentioned above, asymmetric detuning plays an important role in two-qubit entanglement. It is worth studying the effects of asymmetric detuning on the entanglement among multiple qubits.

First, the situation of three qubits is considered. For simplicity, the driving field is resonant with the

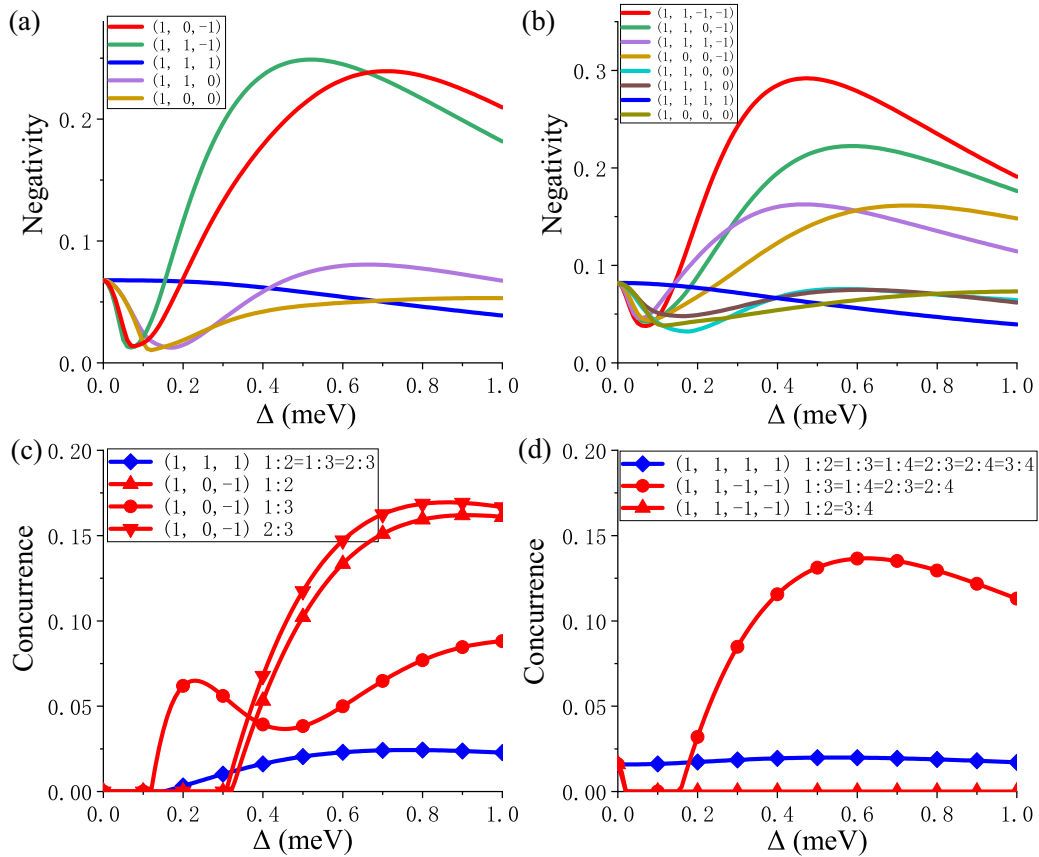


FIG. 3. (a) and (b) Steady-state negativity and (c) and (d) pairwise concurrence ($i : j$ denotes the concurrence of the i th qubit and the j th qubit) as a function of detuning Δ under certain symmetry for three-qubit (left) and four-qubit systems (right). The radius of the nanosphere is $r_a = 16.5$ nm, and the distances between the qubits and the nanosphere are $r_i = 22$ nm (direct dipole-dipole interactions between qubits can be ignored for three-qubit and four-qubit cases). Spontaneous emission rates are $\gamma_i = 0.05$ meV. Rabi frequency $\eta_i = 0.5$ meV.

nanosphere, and the qubits are placed at the vertices of an equilateral triangle whose center coincides with the nanosphere. Furthermore, for practical reasons, the detuning of qubits is limited by a certain symmetry: each Δ_i (for $i = 1, 2, 3$) is either $\pm\Delta$ or zero, where Δ is a variable. Meanwhile, when other parameters remain unchanged, the entanglement behaviors of $\Delta_1 = \Delta_a, \Delta_2 = \Delta_b, \Delta_3 = \Delta_c$ and $\Delta_1 = -\Delta_a, \Delta_2 = -\Delta_b, \Delta_3 = -\Delta_c$ are almost the same (which may be due to some nonstrict symmetries of the system). Therefore, they are treated as the same combination in our discussion below (a similar phenomenon occurs in the four-qubit system). Since these three qubits are equivalent except for detunings, there are only five different detuning combinations: $(1, 0, -1)_3$, $(1, 1, -1)_3$, $(1, 1, 1)_3$, $(1, 1, 0)_3$, and $(1, 0, 0)_3$, where $(i, j, k)_3$ refers to $\Delta_1 = i\Delta, \Delta_2 = j\Delta, \Delta_3 = k\Delta$. Figure 3(a) illustrates the behaviors of negativity when Δ varies from 0 to 1 meV. Among these five combinations, the negativity of $(1, 0, -1)_3$ and $(1, 1, -1)_3$ when the detunings are not zero is significantly larger than when all qubits are resonant with the driving field ($\Delta_i = 0$), while others are close to the resonant condition. Actually, both $(1, 0, -1)_3$ and $(1, 1, -1)_3$ have one pair of qubits whose detunings are antisymmetric, which is the key for entanglement enhancement. Also, Fig. 3(c) shows the pairwise concurrence under the variation of Δ for special combinations: symmetric detuning $(1, 1, 1)_3$

and semiantisymmetric detuning $(1, 0, -1)_3$. Pairwise concurrence and negativity have some common behaviors. For example, in the symmetric detuning case, both negativity and concurrence are robust under the variation of Δ , and in the semiantisymmetric detuning case, proper detunings would maximize the entanglement. A noteworthy phenomenon is that under the resonant condition (each $\Delta_i = 0$), the steady state is fully tripartite entangled as its negativity is greater than zero, while the concurrence of each pair of qubits is zero.

Next, the case of four qubits is discussed. The driving field is still resonant with the nanosphere, and the qubits are placed at the vertices of a square whose center coincides with the center of the nanosphere. If direct dipole-dipole interaction can be ignored (which is true in the parameter region discussed in this paper), the four qubits are equivalent except for their detunings. By further limiting each Δ_i (for $i = 1, 2, 3$) so that it is either $\pm\Delta$ or zero, the truly different detuning combinations are $(1, 1, -1, -1)_4$, $(1, 1, 0, -1)_4$, $(1, 1, 1, -1)_4$, $(1, 0, 0, -1)_4$, $(1, 0, 0, -1)_4$, $(1, 1, 1, 0)_4$, $(1, 1, 1, 1)_4$, and $(1, 0, 0, 0)_4$, where $(i, j, k, l)_4$ refers to $\Delta_1 = i\Delta, \Delta_2 = j\Delta, \Delta_3 = k\Delta, \Delta_4 = l\Delta$. Figure 3(b) illustrates the behaviors of negativity for Δ in the range 0–1 meV. Among the eight combinations, $(1, 1, -1, -1)_4$ provides the largest global entanglement enhancement compared to the resonance case; $(1, 1, 0, -1)_4$, $(1, 1, 1, -1)_4$, and $(1, 0, 0, -1)_4$ are second. Other combinations do not provide significant entanglement

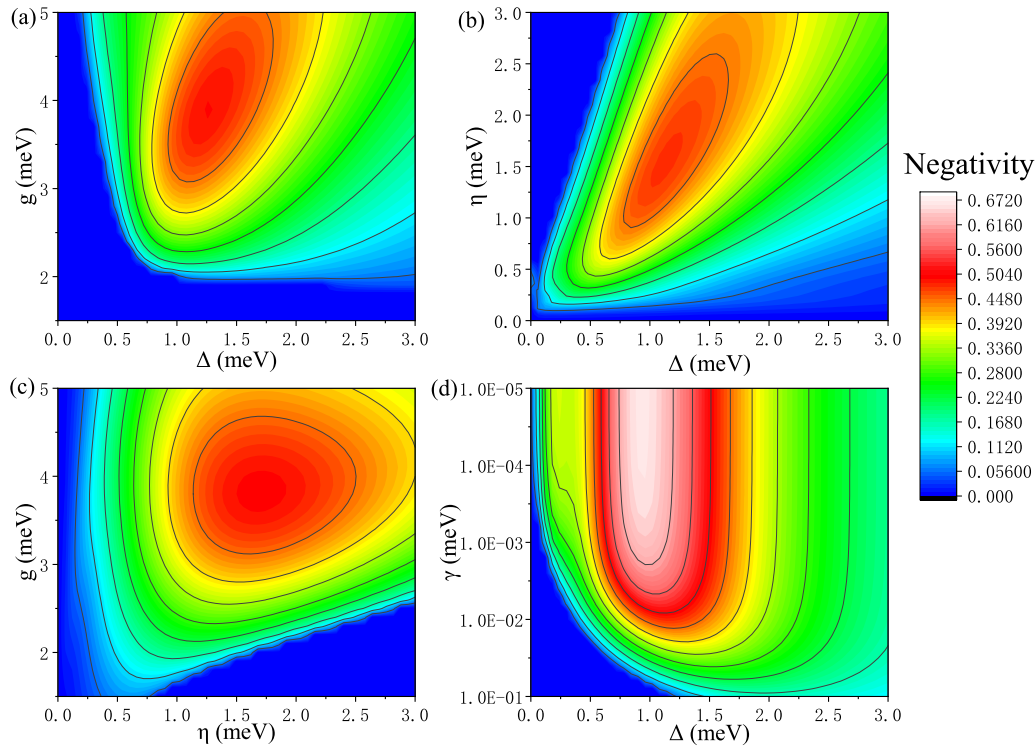


FIG. 4. Steady-state negativity as a function of (a) the coupling constant g and detuning Δ , (b) Rabi frequency η and detuning Δ , (c) the coupling constant g and Rabi frequency η , and (d) the vacuum spontaneous emission rate γ and detuning Δ . Each panel demonstrates the variation of two parameters, and the other two parameters are set to be unchanged. Numerical values of unchanged parameters are set as follows: $\Delta = 1.2$ meV, $\eta = 1.6$ meV, $g = 3.4$ meV, and $\gamma = 10^{-2}$ meV.

enhancement. This phenomenon can be attributed to the number of pairs of qubits whose detunings are antisymmetric. The combination $(1, 1, -1, -1)_4$ has two pairs of antisymmetric detunings qubits, and $(1, 1, 0, -1)_4$, $(1, 1, 1, -1)_4$, and $(1, 0, 0, -1)_4$ each have one pair. It has been shown that in two-qubit systems, antisymmetric detuning ($\Delta_1 = -\Delta_2$) can provide maximum entanglement [22–24], while in multiqubit systems, the number of pairs of antisymmetric detuning qubits should also be taken into account.

Furthermore, the behaviors of local entanglement are depicted in Fig. 3(d), including pairwise concurrence for symmetric detuning $(1, 1, 1, 1)_4$ and semiantisymmetric detuning $(1, 1, -1, -1)$. For the case of symmetric detuning, each pair of qubits forms weak but robust entanglement. In contrast, for the semiantisymmetric detuning case, those pairs of qubits with symmetric detunings could hardly entangle (e.g., 1:2), while the local entanglement of antisymmetric detuning qubits strongly increases under appropriate detuning (e.g., 1:3).

C. Robustness of multiqubit entanglement

The strength of multiqubit entanglement is subjected to the variation of those control parameters. Therefore, it is important to analyze the robustness of the system, that is, the sensitivity of entanglement against the variation of the control parameters which might be caused by imperfections in the experiment. For simplicity, only three-qubit entanglement is considered. Furthermore, all the parameters except detuning

are set to be symmetric: $\eta_i = \eta$, $g_i = g$, and $\gamma_i = \gamma$, which can be realized in a three-qubit system. We set parameters except detuning symmetric because previous researchers have revealed that symmetric parameters can maximize entanglement in two-qubit systems [22,23]. On the other hand, as shown in Sec. III C, asymmetric detuning can significantly enhance entanglement. Thus, the detuning combination $(1, 0, -1)_3$, where $\Delta_1 = -\Delta_3 = \Delta$, $\Delta_2 = 0$, is chosen in the analysis for robustness.

The entanglement under the variation of Δ , η , g , and γ is demonstrated in Fig. 4. Even though fine regulation of the control parameters is needed to obtain the maximum entanglement, it is quite robust under a small deviation of the perfect case. The asymmetric detuning Δ plays an important role in the formation of entanglement. However, when the detuning is large enough, the entanglement decreases as the detuning increases, which has been discovered in two-qubit systems [24]. The coupling constant g has a similar behavior: there is no entanglement when coupling is zero, while the entanglement slowly decreases as g increases when the coupling is large enough. In our effective model, the couplings between the plasmon and qubits can be viewed as a modification of direct dipole coupling among qubits [Eq. (9)]. Although the qubits are placed as far apart as possible so that direct dipole coupling can be ignored in our discussion above, the direct dipole coupling could have a significant effect when the qubits are placed close to each other (e.g., the number of qubits increases). The vacuum spontaneous emission rate γ of qubits, which can be viewed as a kind of dissipation, has

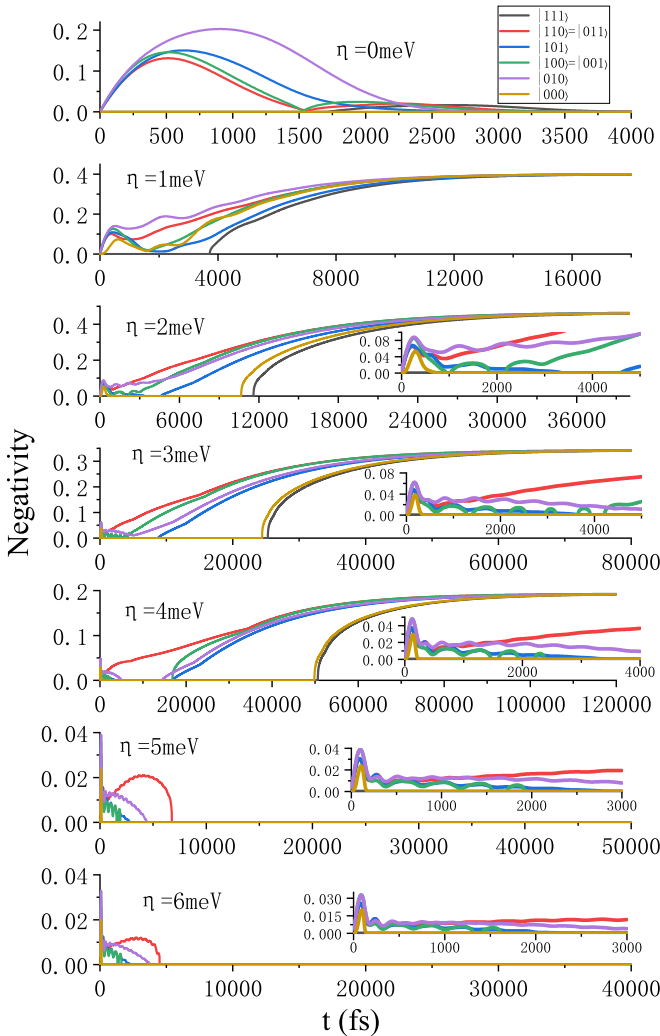


FIG. 5. The dynamics of three-qubit entanglement under different strengths of the driving field. The colors of different lines represent different initial states. The driving field is resonant with the plasmon mode. Here $\Delta_1 = -\Delta_3 = 1.2$ meV, $\Delta_2 = 0$, $g_i = 3.4$ meV, $\gamma_i = 10^{-2}$ meV, and $\eta_i = \eta$.

a negative effect on entanglement. It is worth noting that in the weak-dissipation regime ($\gamma < 10^{-4}$ meV), the variation of γ hardly affects the negativity of the system. The effect of the strength of the driving field (Rabi frequency) is the most interesting. There is no entanglement when $\eta = 0$, which is obvious because dissipation could make the system eventually evolve to the ground state, which is a separable state. A certain strength of the driving field is a necessary condition for entanglement; however, negativity quickly decreases to zero as the strength of the driving field increases when η is large enough (compared to Δ and g). Even though the steady-state negativity is zero both when the driving field is absent and when the driving field is large, the dynamics of entanglement evolution are quite different, which is discussed in Sec. III D. Actually, there would be sudden death when η/g and η/Δ are both large enough. In conclusion, the strength of entanglement under variation of the parameters shares many effects with the two-qubit system.

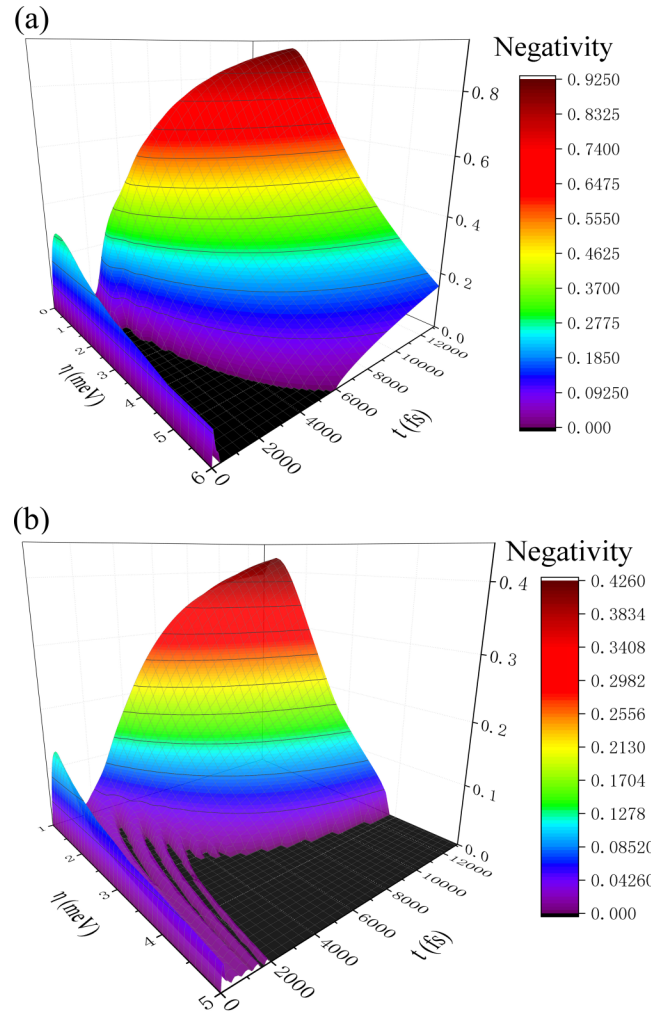


FIG. 6. Negativity as a function of time and the strength of driving field of (a) a two-qubit system and (b) a three-qubit system. The initial states are set to be $|100\rangle$. The driving field is resonant with the plasmon mode. Here $g_i = 3.4$ meV, $\gamma_i = 10^{-2}$ meV, and $\eta_i = \eta$ in both panels, and $\Delta_1 = -\Delta_2 = 1.2$ meV in (a) and $\Delta_1 = -\Delta_3 = 1.2$ meV, $\Delta_2 = 0$ in (b).

D. Sudden death induced by the driving field

ESD is an important manifestation occurring in the entanglement evolution. Here the effect of the driving field on the dynamics of entanglement evolution is analyzed. Negativity as a function of time under different strengths of the driving field is shown in Figs. 5 and 6. Both the zero-driving field ($\eta = 0$ meV) and large-driving field ($\eta > 5$ meV) have a zero steady-state negativity. However, the dynamics of these two situations are not the same. In the case that the driving field is absent, negativity decreases exponentially and towards zero smoothly (unless the initial state is the ground state). However, for the large driving field, negativity would reach zero at a finite time (usually with a discontinuous first derivative) whatever the initial state is, which could be viewed as a kind of sudden death. This kind of entanglement sudden death could be theoretically derived for a two-qubit system, which is shown in the Appendix. One of the most interesting phenomena happens when the driving field is at the right

strength ($\eta \approx 3\text{--}4$ meV): the entanglement disappears at a finite time; however, it revives and reaches its nonzero steady value when $t \rightarrow \infty$.

IV. CONCLUSION

In summary, we studied multiqubit dissipative-driving entanglement generated by a plasmonic system. A simple plasmonic structure composed of a metal nanosphere and multiple qubits was proposed; the dissipation in the system is modeled by Linblad's equation, and an effective model for weak-detuning and weak-coupling mechanisms was derived. Using the effective model, we studied the effects of asymmetric qubit detuning on entanglement. The antisymmetric detunings of a pair of qubits greatly facilitates entanglement compared to resonance. In addition, more pairs of qubits with antisymmetric detunings can achieve even stronger steady-state entanglement. At the same time, the robustness of a three-qubit entanglement system was analyzed, and we found that the proper detuning, coupling constant, and driving field strength could lead to the maximum entanglement value, while the vacuum spontaneous decay rate has a negative influence on the entanglement. Finally, both analytical and numerical calculation indicated that sudden death and revival occur when the driving field is large enough. Our model reveals many phenomena that are consistent with two-qubit entanglement and has great potential for studying multiqubit entanglement phenomena.

ACKNOWLEDGMENTS

This work is supported by the National Key Research and Development Program of China (Grant No. 2017YFA0205700), the National Basic Research Program of China (Grants No. 2015CB932403, No. 2017YFA0206000), the National Science Foundation of China (Grants No. 11674012, No. 61521004, No. 21790364, No. 61422501, and No. 11374023), the Beijing Natural Science Foundation (Grants No. Z180011 and No. L140007), the Foundation for the Author of National Excellent Doctoral Dissertation of China (Grant No. 201420), and the National Program for Support of Top-notch Young Professionals (Grant No. W02070003).

APPENDIX: THEORETICAL DERIVATION OF ENTANGLEMENT SUDDEN DEATH IN A TWO-QUBIT SYSTEM

To simplify, two qubits both at resonance are considered: $\tilde{\Delta} = 0$, and $\tilde{\eta}_i = \eta$, $\tilde{J}_{12} = J$, and $\tilde{\gamma}_{ij} = \gamma\delta_{ij}$. The Hamiltonian of two qubits can be presented as follows:

$$H = H_1 \otimes \mathbf{1} + \mathbf{1} \otimes H_2 + H', \quad (\text{A1})$$

where

$$H_i = \begin{pmatrix} 0 & -\eta \\ -\eta & 0 \end{pmatrix}$$

denotes the interaction between the i th qubit and the outer field and

$$H' = -J(\sigma_1^\dagger \sigma_2 + \sigma_1 \sigma_2^\dagger) = \begin{pmatrix} 0 & 0 & 0 & 0 \\ 0 & 0 & -J & 0 \\ 0 & -J & 0 & 0 \\ 0 & 0 & 0 & 0 \end{pmatrix} \quad (\text{A2})$$

denotes the interaction between qubits. If $\tilde{J}_{12} = 0$, which means the two qubits have no interaction with each other, the steady-state density matrix can be solved separately. For the steady-state density matrix equation

$$\frac{d\rho_i}{dt} = i[\rho_i, H] + \frac{\gamma}{2}(2\sigma_i\rho_i\sigma_i^\dagger - \{\sigma_i^\dagger\sigma_i, \rho_i\}) = 0 \quad (\text{A3})$$

the solution is

$$\rho_i = \frac{1}{8\eta^2 + \gamma^2} \begin{pmatrix} 4\eta^2 & 2i\eta\gamma \\ -2i\eta\gamma & 4\eta^2 + \gamma^2 \end{pmatrix}.$$

For the simplicity of further calculation, the unitary transform

$$U = \frac{1}{\sqrt{2}} \begin{pmatrix} 1 & 1 \\ -1 & 1 \end{pmatrix}$$

is applied for all matrices $M \rightarrow U^\dagger M U$ (or, equally, represents those matrices in a new basis). The transformation of some of the matrices above is as follows:

$$\rho_i \rightarrow \frac{1}{2} \begin{pmatrix} 1 & \frac{\gamma(-\gamma + 4i\eta)}{8\eta^2 + \gamma^2} \\ -\frac{\gamma(\gamma + 4i\eta)}{8\eta^2 + \gamma^2} & 1 \end{pmatrix}, \quad (\text{A4})$$

$$H_i = \begin{pmatrix} 0 & -\eta \\ -\eta & 0 \end{pmatrix} \rightarrow \frac{1}{2} \begin{pmatrix} \eta & 0 \\ 0 & -\eta \end{pmatrix}, \quad (\text{A5})$$

$$H' \rightarrow \frac{J}{2} \begin{pmatrix} -1 & 0 & 0 & 1 \\ 0 & 1 & -1 & 0 \\ 0 & -1 & 1 & 0 \\ 1 & 0 & 0 & -1 \end{pmatrix}, \quad (\text{A6})$$

where the unitary transformation for H' actually means $H' \rightarrow (U^\dagger \otimes U^\dagger)H'(U \otimes U)$. Suppose $J = 0$; then $\rho = \rho_1 \otimes \rho_2$ would be the solution for the steady-state density matrix. For $J \neq 0$, H' is treated as a perturbation in the limit $\eta \rightarrow \infty$, while $\rho = \rho_1 \otimes \rho_2 + \rho'$ and ρ' is the correction for ρ (ρ may not be normalized). From the steady-state equation for the density matrix

$$\frac{d\rho}{dt} = i[\rho_1 \otimes \rho_2 + \rho', H_1 \otimes \mathbf{1} + \mathbf{1} \otimes H_2 + H'] + \Gamma(\rho_1 \otimes \rho_2 + \rho') = 0 \quad (\text{A7})$$

and is simplified by Eq. (A3) ($H_1 + H_2$ denotes $H_1 \otimes \mathbf{1} + \mathbf{1} \otimes H_2$),

$$i[\rho', H_1 + H_2] + i[\rho_1 \otimes \rho_2, H'] + i[\rho', H'] + \Gamma(\rho') = 0. \quad (\text{A8})$$

In the limit where $\eta \rightarrow \infty$, γ/η and J/η are treated as small quantities. Thus, while ignoring the higher-order term in Eq. (A8), the equation of the first-order modification for ρ is

$$[\rho', H_1 + H_2] + [\rho_1 \otimes \rho_2, H'] = 0. \quad (\text{A9})$$

The matrix representations for $H_1 + H_2$ and $\rho_1 \otimes \rho_2$ are (ignoring the higher-order term)

$$H_1 + H_2 = 2\eta \begin{pmatrix} 1 & 0 & 0 & 0 \\ 0 & 0 & 0 & 0 \\ 0 & 0 & 0 & 0 \\ 0 & 0 & 0 & -1 \end{pmatrix}, \quad (\text{A10})$$

$$\rho_1 \otimes \rho_2 = \frac{1}{4} \mathbf{1}_{4 \times 4} + i \frac{\gamma}{8\eta} \begin{pmatrix} 0 & 1 & 1 & 0 \\ -1 & 0 & 0 & 1 \\ -1 & 0 & 0 & 1 \\ 0 & -1 & -1 & 0 \end{pmatrix}, \quad (\text{A11})$$

the solution for ρ' is

$$\rho' = i \frac{\gamma g}{32\eta^2} \begin{pmatrix} 0 & -1 & -1 & 0 \\ 1 & 0 & 0 & 1 \\ 1 & 0 & 0 & 1 \\ 0 & -1 & -1 & 0 \end{pmatrix}, \quad (\text{A12})$$

and the first-order correction of ρ is

$$\rho = \frac{1}{4} \mathbf{1}_{4 \times 4} + i \begin{pmatrix} 0 & a-b & a-b & 0 \\ -a+b & 0 & 0 & a+b \\ -a+b & 0 & 0 & a+b \\ 0 & -a-b & -a-b & 0 \end{pmatrix}, \quad (\text{A13})$$

where

$$a = \frac{\gamma}{8\eta}, \quad b = \frac{\gamma J}{32\eta^2}. \quad (\text{A14})$$

To quantify its entanglement, concurrence is used as an entanglement criterion. In order to calculate concurrence, the eigenvalues of $\sqrt{\rho\tilde{\rho}}$ (or, equivalently, the square root of the eigenvalues of $\rho\tilde{\rho}$) are needed.

After some calculation, it is found that

$$\rho\tilde{\rho} = \left(\frac{1}{16} - 2a^2 + 2b^2 \right) \mathbf{1}_{4 \times 4} + \begin{pmatrix} 0 & -ib/2 & -ib/2 & 2(a+b)^2 \\ ib/2 & 0 & 2(b^2 - a^2) & ib/2 \\ ib/2 & 2(b^2 - a^2) & 0 & ib/2 \\ 2(a-b)^2 & -ib/2 & -ib/2 & 0 \end{pmatrix}. \quad (\text{A15})$$

The eigenvalues of $\rho\tilde{\rho}$ are $(\frac{1}{16} - 2a^2 + 2b^2)$ plus the eigenvalues of the second term in Eq. (A15). In order to obtain the eigenvalues of the second term in Eq. (A15), another unitary transformation,

$$U_1 = \begin{pmatrix} 0 & 1 & 1 & 0 \\ 1 & 0 & 0 & 1 \\ -1 & 0 & 0 & 1 \\ 0 & -1 & 1 & 0 \end{pmatrix},$$

is applied, and the second term in Eq. (A15) becomes

$$\begin{pmatrix} 2a^2 - 2b^2 & 0 & 0 & 0 \\ 0 & -2a^2 - 2b^2 & -4ab & 0 \\ 0 & 4ab & 2a^2 + 2b^2 & -ib \\ 0 & 0 & ib & -2a^2 + 2b^2 \end{pmatrix}. \quad (\text{A16})$$

We define e_i ($i = 1, 2, 3, 4$) as the basis of the matrices. There are no cross terms between e_1 and other e_i ; therefore, $2a^2 - 2b^2$ is one of the eigenvalues of Eq. (A16). Notice that a and b are small quantities, and the cross term between e_2 and e_3 has the same order as the diagonal term of e_2 , which will give a higher order of shift to the eigenvalues; thus, $-2a^2 - 2b^2$ is an approximate eigenvalue of Eq. (A16) to second order. The last step to obtain the eigenvalues of $\rho\tilde{\rho}$ is to solve the eigenvalues in the subspace spanned by e_3 and e_4 ; the eigenvalues are $2b^2 \pm \sqrt{4a^4 + b^2}$. In summary, the eigenvalues of $\rho\tilde{\rho}$ are (in order of largest to smallest) $\frac{1}{16} - 2a^2 + 4b^2 + \sqrt{4a^4 + b^2}$, $\frac{1}{16} - 2a^2 + 4b^2 - \sqrt{4a^4 + b^2}$, $\frac{1}{16}$, and $\frac{1}{16} - 4a^2$. After taking their square root, the concurrence of the system can be written as

$$C = \max\{0, \lambda_1 - \lambda_2 - \lambda_3 - \lambda_4\},$$

$$\lambda_1 - \lambda_2 - \lambda_3 - \lambda_4 = \sqrt{\frac{1}{16} - 2a^2 + 4b^2 + \sqrt{4a^4 + b^2}} - \sqrt{\frac{1}{16} - 2a^2 + 4b^2 - \sqrt{4a^4 + b^2}} - \frac{1}{4} - \sqrt{\frac{1}{16} - 2a^2 + 2b^2}. \quad (\text{A17})$$

Notice that for a proper number of $a > 0$ and $b > 0$, the concurrence of the two qubits could be larger than zero. However, for a large enough η (a and b are small enough), $\lambda_1 - \lambda_2 - \lambda_3 - \lambda_4$ would be lower than zero, which means the steady state will have no entanglement. Moreover, if the initial state is prepared as an entangled state, $C = \lambda_1 - \lambda_2 - \lambda_3 - \lambda_4 > 0$ at $t = 0$. The evolution of $\lambda_1 - \lambda_2 - \lambda_3 - \lambda_4$ should be a continuous function of t ; hence, there must exist a limit time t when $C = \lambda_1 - \lambda_2 - \lambda_3 - \lambda_4 = 0$. The entanglement becomes zero in a finite time, which is the sudden death induced by the driving field.

[1] M. A. Nielsen and I. L. Chuang, *Quantum Computation and Quantum Information* (Cambridge University Press, Cambridge, 2010).

[2] S. J. Devitt, W. J. Munro, and K. Nemoto, *Rep. Prog. Phys.* **76**, 076001 (2013).

[3] A. Ekert and R. Jozsa, *Rev. Mod. Phys.* **68**, 733 (1996).

- [4] Z.-K. Zhou, J. Liu, Y. Bao, L. Wu, C. E. Png, X.-H. Wang, and C.-W. Qiu, *Prog. Quantum Electron.* **65**, 1 (2019).
- [5] M. O. Scully and M. S. Zubairy, *Quantum Optics* (Cambridge University Press, Cambridge, 1997).
- [6] S. P. Walborn, M. O. Terra Cunha, S. Pádua, and C. H. Monken, *Phys. Rev. A* **65**, 033818 (2002).
- [7] M. Hensen, T. Heilpern, S. K. Gray, and W. Pfeiffer, *ACS Photonics* **5**, 240 (2018).
- [8] M. S. Tame, K. R. McEnery, S. K. Özdemir, J. Lee, S. A. Maier, and M. S. Kim, *Nat. Phys.* **9**, 329 (2013).
- [9] J. M. Fitzgerald, P. Narang, R. V. Craster, S. A. Maier, and V. Giannini, *Proc. IEEE* **104**, 2307 (2016).
- [10] S. Bozhevolnyi and N. Mortensen, *Nanophotonics* **6**, 1185 (2017).
- [11] P. Törmä and W. L. Barnes, *Rep. Prog. Phys.* **78**, 013901 (2014).
- [12] J. del Pino, J. Feist, F. J. García-Vidal, and J. J. García-Ripoll, *Phys. Rev. Lett.* **112**, 216805 (2014).
- [13] A. Gonzalez-Tudela, D. Martín-Cano, E. Moreno, L. Martín-Moreno, C. Tejedor, and F. J. Garcia-Vidal, *Phys. Rev. Lett.* **106**, 020501 (2011).
- [14] D. Martín-Cano, A. González-Tudela, L. Martín-Moreno, F. J. García-Vidal, C. Tejedor, and E. Moreno, *Phys. Rev. B* **84**, 235306 (2011).
- [15] A. González-Tudela and D. Porras, *Phys. Rev. Lett.* **110**, 080502 (2013).
- [16] I. M. Mirza and J. C. Schotland, *Phys. Rev. A* **94**, 012302 (2016).
- [17] J. Ren, T. Wu, and X. Zhang, *Sci. Rep.* **5**, 13941 (2015).
- [18] M. Otten, R. A. Shah, N. F. Scherer, M. Min, M. Pelton, and S. K. Gray, *Phys. Rev. B* **92**, 125432 (2015).
- [19] M. Otten, J. Larson, M. Min, S. M. Wild, M. Pelton, and S. K. Gray, *Phys. Rev. A* **94**, 022312 (2016).
- [20] M. Otten, S. K. Gray, and G. V. Kolmakov, *Phys. Rev. A* **99**, 032339 (2019).
- [21] J. B. Khurgin, *Nat. Nanotechnol.* **10**, 2 (2015).
- [22] J. Hou, K. Slowik, F. Lederer, and C. Rockstuhl, *Phys. Rev. B* **89**, 235413 (2014).
- [23] E. Dumitrescu and B. Lawrie, *Phys. Rev. A* **96**, 053826 (2017).
- [24] F. Zhang, D. Zhao, Y. Gu, H. Chen, X. Hu, and Q. Gong, *J. Appl. Phys.* **121**, 203105 (2017).
- [25] F. Zhang, D. Zhao, X. Hu, Q. Gong, and Y. Gu, *J. Phys. B* **52**, 115402 (2019).
- [26] F. Zhang, J. Ren, X. Duan, Z. Chen, Q. Gong, and Y. Gu, *J. Phys.: Condens. Matter* **30**, 305302 (2018).
- [27] N. Iliopoulos, I. Thanopoulos, V. Yannopoulos, and E. Paspalakis, *Phys. Rev. B* **97**, 115402 (2018).
- [28] M. Qurban, M. Ikram, G.-Q. Ge, and M. S. Zubairy, *J. Phys. B* **51**, 155502 (2018).
- [29] F. Dieleman, M. S. Tame, Y. Sonnefraud, M. S. Kim, and S. A. Maier, *Nano Lett.* **17**, 7455 (2017).
- [30] K. V. Nerkararyan and S. I. Bozhevolnyi, *Phys. Rev. B* **92**, 045410 (2015).
- [31] S. Haroche and D. Kleppner, *Phys. Today* **42**(1), 24 (1989).
- [32] W. K. Wootters, *Phys. Rev. Lett.* **80**, 2245 (1998).
- [33] C. Sabín and G. García-Alcaine, *Eur. Phys. J. D* **48**, 435 (2008).
- [34] G. Vidal and R. F. Werner, *Phys. Rev. A* **65**, 032314 (2002).